Domain III of the *T. thermophilus* 23S rRNA folds independently to a near-native state

Shreyas S. Athavale, J. Jared Gossett, Chiaolong Hsiao, et al.

RNA 2012 18: 752-758 originally published online February 14, 2012
Access the most recent version at doi:10.1261/rna.030692.111

Domain III of the *T. thermophilus* 23S rRNA folds independently to a near-native state

SHREYAS S. ATHAVALE,[1] J. JARED GOSSETT,[1] CHIAOLONG HSIAO,[2] JESSICA C. BOWMAN,[2] ERIC O'NEILL,[2] ELI HERSHKOVITZ,[2] THANAWADEE PREEPREM,[1] NICHOLAS V. HUD,[2] ROGER M. WARTELL,[1] STEPHEN C. HARVEY,[1,2] and LOREN DEAN WILLIAMS[2,3]

[1]School of Biology and [2]School of Chemistry and Biochemistry, Georgia Institute of Technology, Atlanta, Georgia 30332, USA

ABSTRACT

The three-dimensional structure of the ribosomal large subunit (LSU) reveals a single morphological element, although the 23S rRNA is contained in six secondary structure domains. Based upon maps of inter- and intra-domain interactions and proposed evolutionary pathways of development, we hypothesize that Domain III is a truly independent structural domain of the LSU. Domain III is primarily stabilized by intra-domain interactions, negligibly perturbed by inter-domain interactions, and is not penetrated by ribosomal proteins or other rRNA. We have probed the structure of Domain III rRNA alone and when contained within the intact 23S rRNA using SHAPE (selective 2′-hydroxyl acylation analyzed by primer extension), in the absence and presence of magnesium. The combined results support the hypothesis that Domain III alone folds to a near-native state with secondary structure, intra-domain tertiary interactions, and inter-domain interactions that are independent of whether or not it is embedded in the intact 23S rRNA or within the LSU. The data presented support previous suggestions that Domain III was added relatively late in ribosomal evolution.

Keywords: ribosome; large subunit; independent fold; ribosomal evolution; SHAPE

INTRODUCTION

The ribosome is our most direct macromolecular connection to the distant evolutionary past and to early life (Woese 2001; Wolf and Koonin 2007; Smith et al. 2008; Bokov and Steinberg 2009; Hsiao et al. 2009; Belousoff et al. 2010; Fox 2010). The ribosome is believed to have emerged from the "RNA world" (Rich 1962; Woese 1967; Crick 1968; Orgel 1968; Gilbert 1986) following an evolutionary pathway that preserved ribosomal RNAs as central players in peptide bond formation and decoding (Noller et al. 1992; Ban et al. 2000; Nissen et al. 2000; Harms et al. 2001; Ogle et al. 2001; Yusupov et al. 2001; Schuwirth et al. 2005; Selmer et al. 2006). Understanding the origin and evolution of rRNA is a key to understanding the early evolution of life on earth.

The ribosome is made of a small subunit (SSU) and a large subunit (LSU). The SSU in bacteria and archaea contains a single RNA molecule, the 16S rRNA. Phylogenetic studies by Woese et al. (1980) revealed three major and one minor secondary structural domains (2° domains) of the 16S rRNA. These 2° domains are segregated into independent and autonomous three-dimensional domains (3D domains) in the assembled SSU. Each 2° domain of the 16S rRNA folds and assembles with the appropriate ribosomal proteins into a 3D domain, independent of other 2° domains (Weitzmann et al. 1993; Samaha et al. 1994; Agalarov et al. 1999). One 3D domain is called the head and others are called the body and the platform (Brimacombe et al. 1983; Wimberly et al. 2000). The head, body, and platform domains of the SSU have direct functional significance, moving independently during translation (Noller 2005). These 3D domains may also have evolutionary significance. The domain is the evolutionary unit of protein evolution (Campbell and Downing 1994; Fong et al. 2007). Protein domains are modular units that are combined and recombined over evolution to achieve various functions. It is conceivable that the 3D domains of the SSU played analogous evolutionary roles, but on a more ancient timeframe. If so, then the 3D domains of the SSU may have been recruited to the ribosome, from prior functional roles.

The LSU in bacteria and archaea is made up of a 23S rRNA and a much smaller 5S rRNA. The 23S rRNA con-

[3]**Corresponding author.**
E-mail loren.williams@chemistry.gatech.edu.

Article published online ahead of print. Article and publication date are at http://www.rnajournal.org/cgi/doi/10.1261/rna.030692.111.

tains six 2° domains (Fig. 1A; Noller et al. 1981). Although these 2° domains are well-defined in the secondary structure, in three dimensions the LSU appears monolithic (Tumminia et al. 1994; Ban et al. 2000; Yusupov et al. 2001). It has been suggested that, unlike in the SSU, the 2° domains in the LSU do not correspond to 3D domains.

Questions naturally arise as to whether the architectures and early evolution of the SSU and the LSU are fundamentally different, and if so, why? Do isolated 2° domains of the 16S rRNA but not the 23S rRNA act as 3D domains and fold to near-native 3D structures? How are the 2° domains of the 16S and 23S rRNAs related to 3D structure, function, and evolution of the ribosome?

Here we experimentally probe the domain structure of the LSU. We show that one isolated 2° domain of the 23S rRNA can fold to a near-native state in absence of the re-

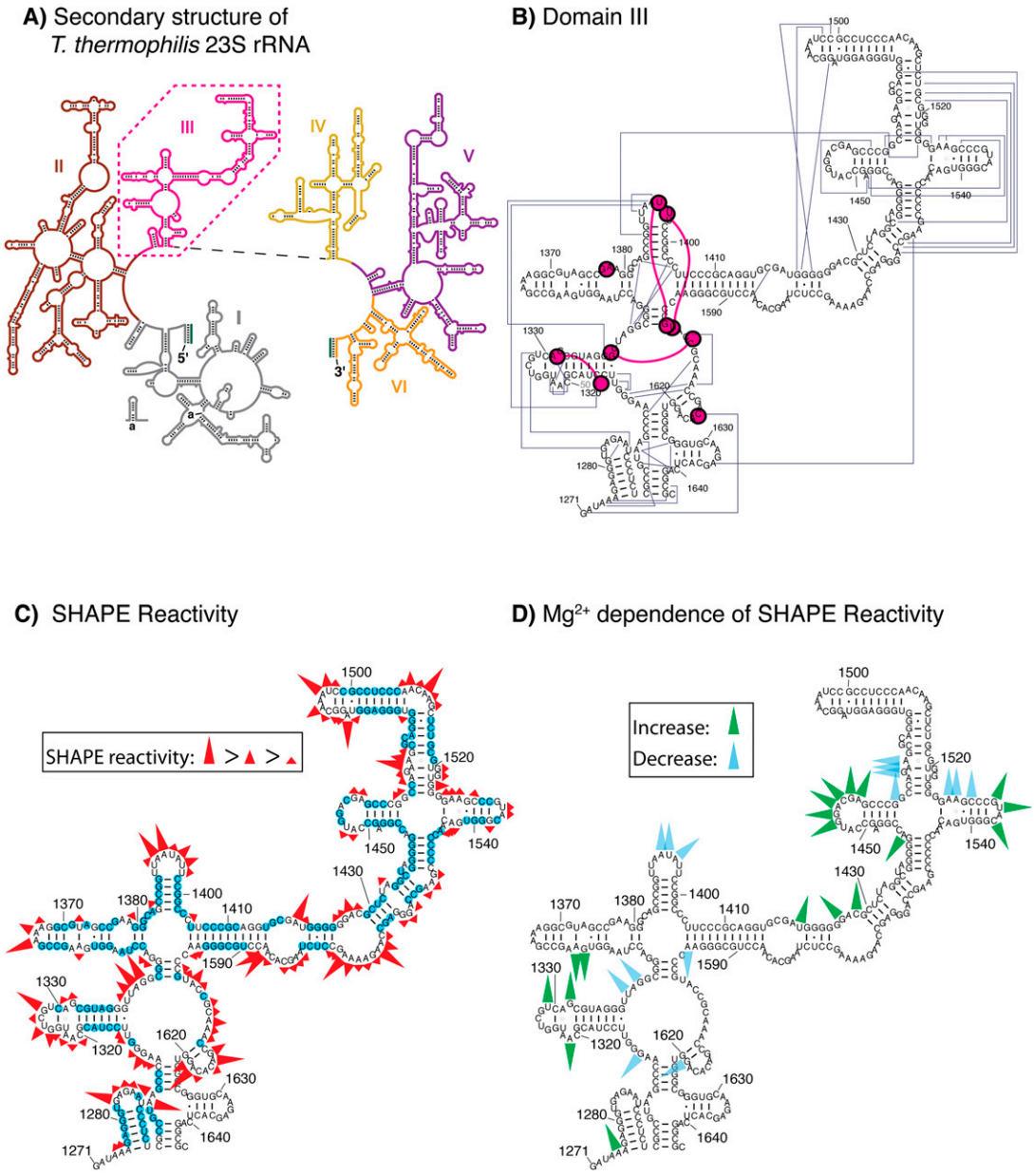

FIGURE 1. (*A*) Secondary structure of the 23S rRNA of the large subunit of *T. thermophilus* (adapted with permission from Harry Noller). The six secondary structural domains of 23S rRNA are shown: Domain I in gray, Domain II in brown, Domain III in pink, Domain IV in yellow, Domain V in purple, and Domain VI in orange. (*B*) Tertiary interactions (dark blue) and phosphate–magnesium–phosphate linkages within Domain III. Each first shell magnesium–phosphate interaction is indicated by a magenta circle. The lines between the circles are the phosphate–magnesium–phosphate linkages. (*C*) SHAPE reactivities for Domain III^{alone} in 250 mM Na^+. The blue nucleotides are unreactive. (*D*) Magnesium-dependent SHAPE reactivities for Domain III^{alone}, observed upon addition of 10 mM Mg^{2+}. Only the nucleotides with the greatest proportional change in reactivity are indicated.

mainder of the LSU, and appears to be a true 3D domain. Our focus here is Domain III of the *Thermus thermophilus* 23S rRNA (Fig. 1B), which is described by Thirumalai and colleagues (Hyeon et al. 2006) as compact and slightly prolate. We use SHAPE (Merino et al. 2005; Wilkinson et al. 2005) to demonstrate that Domain III excised from the 23S rRNA (Domain III^{alone}) folds in a magnesium-dependent fashion to the same basic state as when it is embedded in the intact 23S rRNA (Domain III^{23S}). In this near-native state of Domain III, surface residues appear to be poised with the correct geometry for the inter-domain rRNA–rRNA interactions observed in the structure of the LSU (PDB entry 2J01) (Selmer et al. 2006). Our results are consistent with the structure of Domain III within the LSU where Domain III is compact, and its interactions with other ribosomal components are restricted to its surface (Figs. 2, 3; Supplemental Fig. S1).

RESULTS

SHAPE accurately predicts the canonical secondary structure of Domain III^{alone}

The canonical secondary structure of the 23S rRNA, based on comparative sequence analysis (Yusupov et al. 2001; Cannone et al. 2002), is strongly supported by previous SHAPE experiments (Deigan et al. 2009). As shown by Weeks and colleagues, SHAPE exploits the reactivity of the 2′-hydroxyl groups of RNA with electrophilic chemical probing reagents such as NMIA (*N*-methylisatoic anhydride) or BzCN (benzoyl cyanide) (Merino et al. 2005; Wilkinson et al. 2005). The relative reactivities of the 2′-hydroxyl groups of various nucleotides are sensitive primarily to local RNA flexibility. Consequently, paired nucleotides within helical regions are generally less flexible and less reactive toward SHAPE reagents than unpaired nucleotides.

The close correspondence of our SHAPE data to the canonical secondary structure of Domain III is illustrated in Figure 1C, where SHAPE reactivity of Domain III^{alone} is mapped onto the canonical secondary structure. All SHAPE reactivity data were obtained using NMIA unless otherwise specified. The definition of Domain III used here is conventional and includes residues G1271–G1647 of the 23S rRNA by the *Escherichia coli* numbering scheme (Brosius et al. 1980; Yusupov et al. 2001). These data were obtained in presence of 250 mM Na^+ ions and in the absence of divalent cations. Under these conditions, RNA is expected to assume secondary structure but not necessarily tertiary structure (Brion and Westhof 1997; Draper 2008). Consistent with this tendency, the correspondence between SHAPE reactivities and the secondary structure is very nearly perfect. Nucleotides of Domain III^{alone} were ranked using their absolute SHAPE reactivities relative to A1572 (highest reactivity) and binned into four groups, which are indicated in Figure 1C (see Supplemental Material for a more detailed analysis).

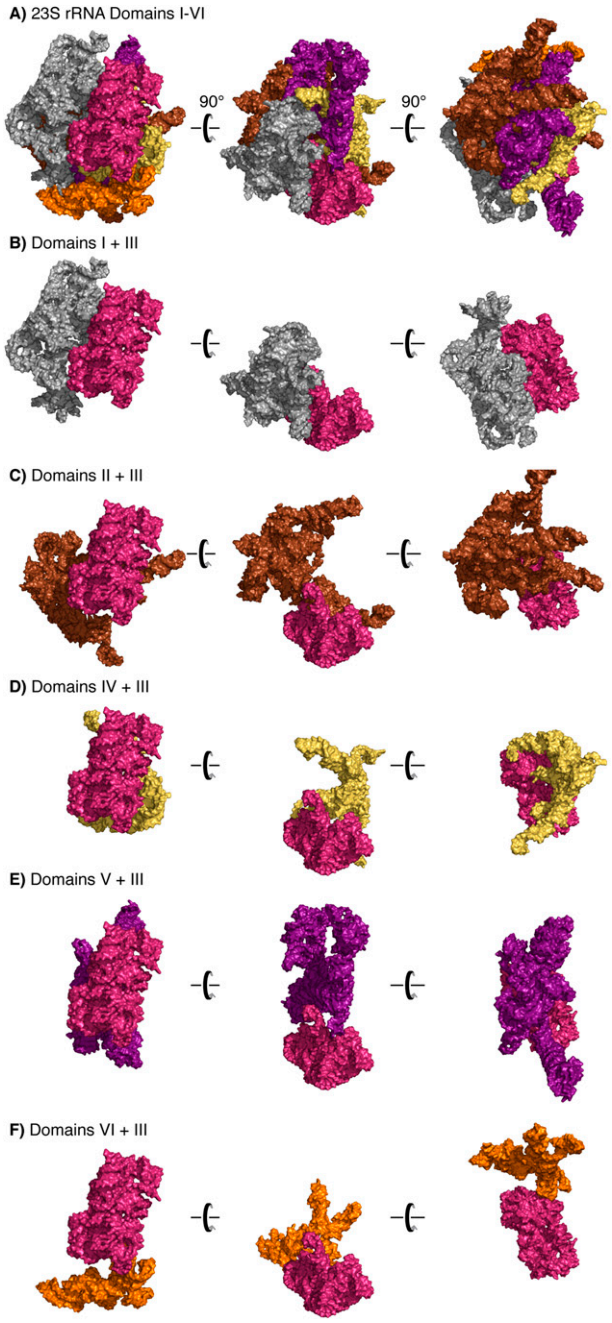

FIGURE 2. Domain III is compact and is not penetrated by other 2° domains. (*A*) All six 2° domains of the 23S rRNA are shown, colored as in Figure 1. Three views, with a relative rotation of 90°, are shown. (*B–F*) Interactions of Domain III with Domains I, II, IV, V, and VI, respectively.

Folding of Domain III^{alone} to a near-native state requires magnesium ions

The folding of RNAs from secondary structure to their native states, containing long-range tertiary interactions, is known to be generally magnesium-dependent (Brion and Westhof 1997; Draper 2008). The native state of Domain III rRNA, as inferred from the 3D structure of the as-

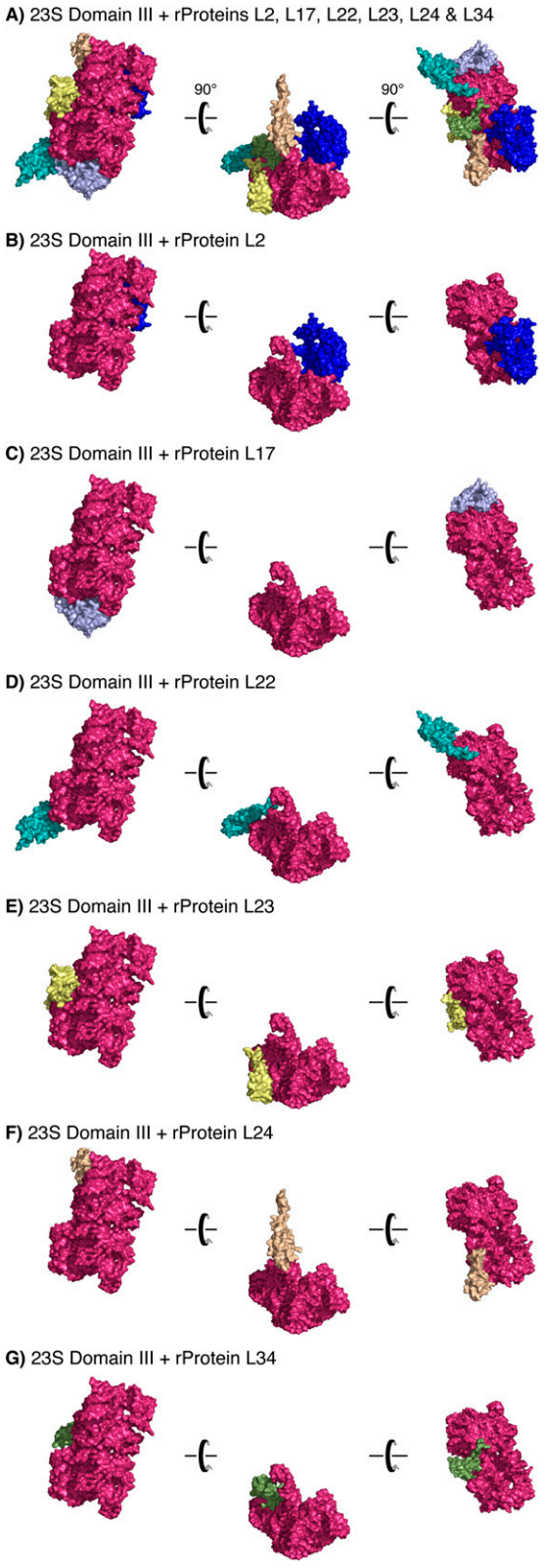

FIGURE 3. Domain III is not penetrated by ribosomal proteins. (*A*) Domain III, colored and oriented as in Figure 2, with rProteins L2 (dark blue), L17 (light blue), L22 (dark green), L23 (yellow), L24 (light brown), and L34 (light green). (*B–G*) Interactions of Domain III with each of these rProteins.

sembled LSU, is stabilized by extensive networks of intra-domain tertiary base–base, base–backbone, and backbone–magnesium–backbone interactions (Fig. 1B). Consistent with this observation, Figure 1D shows that the magnesium-induced changes in SHAPE reactivity of Domain III^{alone} are widely dispersed over Domain III rRNA. The SHAPE reactivities increase at some sites and decrease at others. The nucleotides with SHAPE reactivities that are most sensitive to magnesium are mapped onto the secondary structure in Figure 1D. This magnesium dependence of the SHAPE reactivity reflects (i) specific magnesium binding, (ii) more diffuse interactions of magnesium with the RNA, and (iii) tertiary rRNA–rRNA intra-domain interactions (Supplemental Tables S1, S2). Such magnesium-dependent SHAPE reactivity has previously been demonstrated for tRNA and RNase P (Merino et al. 2005; Mortimer and Weeks 2008).

We used two chemical reagents to verify that the observed changes in reactivity are the result of RNA folding and not from direct modulation of the reagent activity by magnesium. Although SHAPE reactivity of NMIA has been shown to be modestly sensitive to magnesium (Mortimer and Weeks 2007), reactivity of BzCN is independent of magnesium (Mortimer and Weeks 2008). We confirmed that NMIA and BzCN show similar changes in SHAPE reactivity upon addition of magnesium (Supplemental Fig. S2).

The secondary structure of Domain III rRNA is conserved upon excision from the 23S rRNA

Figure 4A shows the SHAPE reactivities of Domain III^{alone} and Domain III^{23S}, both in the absence of magnesium. As illustrated by the overlaid traces, the reactivities are essentially identical along the length of the Domain III sequence. The high degree of similarity suggests that the secondary structure of Domain III^{alone} is the same as Domain III^{23S}.

Mg^{2+}-mediated folding of Domain III to the near-native state is conserved upon excision from the 23S rRNA

In the presence of magnesium ions, the SHAPE reactivities for Domain III^{alone} and Domain III^{23S} are very similar (Fig. 4B). The magnesium-dependent state of Domain III is therefore retained when it is excised from the 23S rRNA. The data also show that inter-domain rRNA–rRNA interactions are disrupted upon excision of Domain III from the 23S rRNA. In presence of magnesium, the SHAPE reactivity of Domain III^{23S} differs subtly from that of Domain III^{alone} (Fig. 4B). The differences are statistically focused at nucleotides involved in inter-domain interactions in the LSU, rather than at other regions of the Domain III rRNA. Of the 33 nucleotides (nt) that report a difference in SHAPE reactivity of ≥40% between Domain III^{23S} and Domain III^{alone} in the presence of magnesium, 25 are seen to be involved in direct inter-domain interactions (<3.4 Å

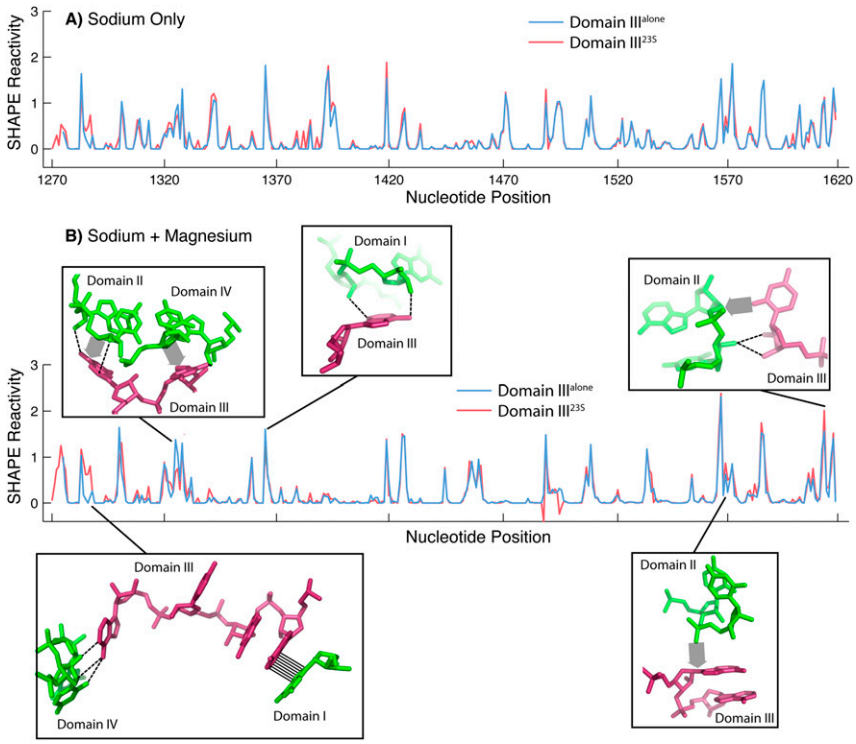

FIGURE 4. SHAPE reactivity for Domain III^{alone} (blue) and Domain III^{23S} (red). The vertical axis represents SHAPE reactivities and the horizontal axis represents nucleotide position using conventional *E. coli* numbering scheme. (*A*) Domain III^{alone} and Domain III^{23S} in 250 mM Na^+. (*B*) Domain III^{alone} and Domain III^{23S} in 250 mM Na^+ and 10 mM Mg^{2+}. The inter-domain interactions between Domain III and Domains I, II, and IV that cause differences in SHAPE reactivity between Domain III^{alone} and Domain III^{23S} are highlighted. Hydrogen bonds are shown by dashed lines, stacking interactions are shown by hashing, and van der Waals contacts are shown by broad shaded arrows.

interatomic distances) in the LSU or are in close proximity to those nucleotides involved in inter-domain interactions. This pattern suggests that Domain III^{alone} folds into a near-native state, and that "insertion" of Domain III into the 23S rRNA (to form Domain III^{23S}) primarily affects the nucleotides involved in inter-domain interactions. A detailed list of other inter-domain interactions is available in Supplemental Tables S3, S4; the tables also indicate if SHAPE detects these interactions.

Specifically, the 3D structure of the LSU shows that A1284 forms base–backbone hydrogen bonds with G489 of Domain I. Nearby A1287 forms base–base stacking interactions with C1648 of Domain IV. As seen in Figure 4B, adding Domain III back into the 23S rRNA changes the SHAPE reactivities of A1284 and A1287. Similar changes in SHAPE reactivities are seen for (i) fragment G1325–G1332, where G1325 forms base–backbone hydrogen bonds with A1269 and C1270 of Domain II, and U1326 forms base–backbone hydrogen bonds with C1648 and G2010 of Domain IV; (ii) A1365, which forms base–backbone hydrogen bonds with G187 of Domain I; (iii) nucleotides G1568–A1570, where A1569 forms van der Waals contacts with C693 of Domain II; and (iv) nucleotides A1616–C1617, where C1617 forms base–backbone and backbone–backbone hydrogen bonds with C749 and A750 of Domain II. This pattern of differential SHAPE reactivity indicates the subtle structural changes that occur when Domain III forms inter-domain interactions with other elements of the 23S rRNA. These inter-domain interactions are disrupted when Domain III is excised from the 23S rRNA, while the intra-domain interactions are conserved.

DISCUSSION

The domain structures of rRNAs have profound implications for folding and function of the ribosome, and early evolution of life. In contrast to the SSU, it has been proposed that the 2° domains of the LSU (Fig. 1A) are melded into a single monolithic unit (Tumminia et al. 1994; Ban et al. 2000; Yusupov et al. 2001). LSU 2° domains are thought to be so highly intertwined and interconnected that they lack distinct structural and functional significance and are not true 3D domains.

Considering the extensive network of intra-domain tertiary interactions of Domain III (Fig. 1B; Supplemental Tables S1, S2) and its isolation from the inter-domain network of molecular interactions within the LSU, we hypothesize that Domain III is a true 3D domain. In contrast, Domain V, which contains the Peptidyl Transferase Center, is extensively networked with other 2° domains. Domain V makes 24 inter-domain A-minor interactions (Bokov and Steinberg 2009). Additionally, Domain V makes six inter-domain magnesium-mediated phosphate–phosphate linkages (Hsiao and Williams 2009). Domain III only makes six A-minor interactions and single magnesium-mediated phosphate–phosphate linkage with other 2° domains.

We present data indicating that Domain III^{alone} adopts a secondary structure that is the same as Domain III^{23S} (Figs. 1C, 4A). The addition of magnesium facilitates folding to a near-native state of both Domain III^{alone} and Domain III^{23S}, with the formation of intra-domain tertiary interactions (Figs. 1D, 4B). The disruption of inter-domain interactions of Domain III is reflected in the subtle but observable changes in SHAPE reactivity when Domain III is excised from the 23S rRNA (i.e., when Domain III^{23S} is converted to Domain III^{alone}) (Fig. 4B). The mapping of these changes in SHAPE reactivity to regions of inter-domain interactions is evidence that Domain III^{alone} and Domain

III^{23S} fold to near-native states. This interpretation is supported by the previous observation that Domain III^{alone} interacts specifically with ribosomal protein L23 (Ostergaard et al. 1998).

In sum it appears that, like the SSU, the LSU also contains some elements of a 3D domain-based architecture, in spite of its monolithic appearance. At least some 2° domains of the 23S rRNA (Domain III) autonomously fold to near-native states apart from the rest of the LSU. Consequently, at least some LSU 2° domains may have played roles similar to SSU 2° domains during the evolutionary development of the ribosome. Previous support for the importance of 3D domains of the LSU is found in the demonstration that Domain I alone is highly structured (Egebjerg et al. 1987). Further, Garret and colleagues have demonstrated that isolated domains of the 23S rRNA are able to form the correct secondary structure and bind to specific ribosomal proteins (Egebjerg et al. 1987; Leffers et al. 1988; Ostergaard et al. 1998).

Evolutionary implications of the domain structure of the Domain III

The ribosome in its present form was well-established at the emergence of the last universal common ancestor of life (LUCA) (Woese 2001; Wolf and Koonin 2007; Smith et al. 2008; Bokov and Steinberg 2009; Hsiao et al. 2009; Belousoff et al. 2010; Fox 2010). There is a consensus that some parts of the ribosome are even older than LUCA, predating the protein world. Parts of Domain V of the 23S rRNA are believed to be among the most ancient parts of the ribosome (Woese 2001; Wolf and Koonin 2007; Smith et al. 2008; Bokov and Steinberg 2009; Hsiao et al. 2009; Belousoff et al. 2010; Fox 2010) while Domain III is thought to be a more recent addition (Hury et al. 2006). The data presented here support the hypothesis that Domain III was added as an intact entity to the ancestral ribosome—assuming that the 3D domain is a unit of ribosomal evolution. This evolutionary model is consistent with the absence of Domain III from certain mitochondrial rRNAs, such as that of *Trypanosoma brucei* (Sloof et al. 1985). Ribosomes in which Domain III is absent may have had this domain deleted by relatively recent evolutionary processes within the mitochondrion, but presumably retained functionality with the assistance of proteins.

MATERIALS AND METHODS

T. thermophilus rRNA transcripts were produced and purified as described in the Supplemental Material.

SHAPE reactions

Magnesium was removed from 25 pmol of Domain III or 23S RNA in 32 μL 1× TE (10 mM Tris-HCl, 1 mM EDTA, pH 8.0) by heating in the presence of magnesium chelating resin (Hampton Research) to 95°C for 3 min, followed by chilling on ice. Thirty-two microliters of Mg^{2+}-free RNA was mixed with 4 μL 10× folding buffer (500 mM HEPES pH 8.0, 2 M sodium acetate pH 8.0) and then incubated at 37°C for 20 min. For RNA folding with Mg^{2+}, the 10× folding buffer contained 500 mM HEPES pH 8.0, 2 M sodium acetate pH 8.0, 100 mM $MgCl_2$.

The folded RNA was divided equally between two tubes. To one tube, 2 μL of 130 mM NMIA (or 800 mM BzCN) in anhydrous DMSO was added, while the other half served as a negative control to which 2 μL pure DMSO was added. The reactions were incubated at 37°C for 1 h with NMIA. The modification reaction using BzCN is complete in a few seconds at room temperature (Mortimer and Weeks 2008). Denaturing SHAPE experiments were performed in 20 mM HEPES pH 8.0 (final concentration) for 4 min at 90°C using 130 mM NMIA in anhydrous DMSO. The modified RNA was purified using RNeasy Mini Kit (Qiagen) and resuspended in 20 μL 1× TE. The recovery after purification was 65%–75%.

A 20-nt long DNA oligomer 5′-CGCGCCTGAGTGCTCTT GCA-3′, that anneals to the 3′-end of Domain III, was used to prime the reverse transcription. The primer was labeled with 6-FAM using a 5′-amino C6 linker (Operon MWG). Twenty microliters of modified RNA was added to 8 pmol of the primer in 10 μL of 1× TE. The RNA-primer solution was heated to 95°C for 1 min and cooled to 30°C over 45 min at a rate of 1.4°C/min. After primer annealing, SuperScript III Reverse Transcriptase buffer (Invitrogen) was added at 30°C. The solution was heated to 55°C for 1 min and reverse transcription was initiated by adding 1 μL (200 U) of SuperScript III Reverse Transcriptase (Invitrogen). The reaction was incubated at 55°C for 2 h and quenched by heating to 70°C for 15 min. Di-deoxy sequencing reactions used unmodified Domain III RNA and 1 mM ddNTPs (TriLink BioTechnologies). One microliter of the reverse transcription reaction mixture was mixed with 0.3 μL ROX-labeled DNA sizing ladder and 8.7 μL of Hi-Di Formamide (Applied Biosystems) in a 96-well plate. The mixture was heated to 95°C for 5 min to denature the cDNAs and resolved on a 3130 Genetic Analyzer (Applied Biosystems) using custom fluorescence spectral calibration. Capillary electrophoresis data were processed as described in the Supplemental Material.

Tertiary interactions

A detailed description of the protocol followed to annotate the intra-domain and inter-domain tertiary interactions observed for Domain III is available in the Supplemental Material.

SUPPLEMENTAL MATERIAL

Supplemental material is available for this article.

ACKNOWLEDGMENTS

This work was supported by the NASA Astrobiology Institute and the Center for Ribosomal Origins and Evolution. We thank Timothy K. Lenz for helpful discussions.

Received October 2, 2011; accepted December 24, 2011.

REFERENCES

Agalarov SC, Selivanova OM, Zheleznyakova EN, Zheleznaya LA, Matvienko NI, Spirin AS. 1999. Independent *in vitro* assembly of all three major morphological parts of the 30S ribosomal subunit of *Thermus thermophilus*. *Eur J Biochem* **266:** 533–537.

Ban N, Nissen P, Hansen J, Moore PB, Steitz TA. 2000. The complete atomic structure of the large ribosomal subunit at 2.4 Å resolution. *Science* **289:** 905–920.

Belousoff MJ, Davidovich C, Zimmerman E, Caspi Y, Wekselman I, Rozenszajn L, Shapira T, Sade-Falk O, Taha L, Bashan A, et al. 2010. Ancient machinery embedded in the contemporary ribosome. *Biochem Soc Trans* **38:** 422–427.

Bokov K, Steinberg SV. 2009. A hierarchical model for evolution of 23S ribosomal RNA. *Nature* **457:** 977–980.

Brimacombe R, Maly P, Zwieb C. 1983. The structure of ribosomal RNA and its organization relative to ribosomal protein. *Prog Nucleic Acid Res Mol Biol* **28:** 1–48.

Brion P, Westhof E. 1997. Hierarchy and dynamics of RNA folding. *Annu Rev Biophys Biomol Struct* **26:** 113–137.

Brosius J, Dull TJ, Noller HF. 1980. Complete nucleotide sequence of a 23S ribosomal RNA gene from *Escherichia coli*. *Proc Natl Acad Sci* **77:** 201–204.

Campbell ID, Downing AK. 1994. Building protein structure and function from modular units. *Trends Biotechnol* **12:** 168–172.

Cannone JJ, Subramanian S, Schnare MN, Collett JR, D'Souza LM, Du Y, Feng B, Lin N, Madabusi LV, Muller KM, et al. 2002. The comparative RNA web (CRW) site: An online database of comparative sequence and structure information for ribosomal, intron, and other RNAs. *BMC Bioinformatics* **3:** 2. doi: 10.1186/1471-2105-3-2.

Crick FH. 1968. The origin of the genetic code. *J Mol Biol* **38:** 367–379.

Deigan KE, Li TW, Mathews DH, Weeks KM. 2009. Accurate SHAPE-directed RNA structure determination. *Proc Natl Acad Sci* **106:** 97–102.

Draper DE. 2008. RNA folding: Thermodynamic and molecular descriptions of the roles of ions. *Biophys J* **95:** 5489–5495.

Egebjerg J, Leffers H, Christensen A, Andersen H, Garrett RA. 1987. Structure and accessibility of domain I of *Escherichia coli* 23S RNA in free RNA, in the L24-RNA complex and in 50S subunits. Implications for ribosomal assembly. *J Mol Biol* **196:** 125–136.

Fong JH, Geer LY, Panchenko AR, Bryant SH. 2007. Modeling the evolution of protein domain architectures using maximum parsimony. *J Mol Biol* **366:** 307–315.

Fox GE. 2010. Origin and evolution of the ribosome. *Cold Spring Harb Perspect Biol* **2:** a003483. doi: 10.1101/cshperspect.a003483.

Gilbert W. 1986. Origin of life: The RNA world. *Nature* **319:** 618.

Harms J, Schluenzen F, Zarivach R, Bashan A, Gat S, Agmon I, Bartels H, Franceschi F, Yonath A. 2001. High resolution structure of the large ribosomal subunit from a mesophilic eubacterium. *Cell* **107:** 679–688.

Hsiao C, Williams LD. 2009. A recurrent magnesium-binding motif provides a framework for the ribosomal peptidyl transferase center. *Nucleic Acids Res* **37:** 3134–3142.

Hsiao C, Mohan S, Kalahar BK, Williams LD. 2009. Peeling the onion: Ribosomes are ancient molecular fossils. *Mol Biol Evol* **26:** 2415–2425.

Hury J, Nagaswamy U, Larios-Sanz M, Fox GE. 2006. Ribosome origins: The relative age of 23S rRNA domains. *Orig Life Evol Biosph* **36:** 421–429.

Hyeon C, Dima RI, Thirumalai D. 2006. Size, shape, and flexibility of RNA structures. *J Chem Phys* **125:** 194905. doi: 10.1063/1.2364190.

Leffers H, Egebjerg J, Andersen A, Christensen T, Garrett RA. 1988. Domain VI of *Escherichia coli* 23S ribosomal RNA. Structure, assembly and function. *J Mol Biol* **204:** 507–522.

Merino EJ, Wilkinson KA, Coughlan JL, Weeks KM. 2005. RNA structure analysis at single nucleotide resolution by selective 2′-hydroxyl acylation and primer extension (SHAPE). *J Am Chem Soc* **127:** 4223–4231.

Mortimer SA, Weeks KM. 2007. A fast-acting reagent for accurate analysis of RNA secondary and tertiary structure by SHAPE chemistry. *J Am Chem Soc* **129:** 4144–4145.

Mortimer SA, Weeks KM. 2008. Time-resolved RNA SHAPE chemistry. *J Am Chem Soc* **130:** 16178–16180.

Nissen P, Hansen J, Ban N, Moore PB, Steitz TA. 2000. The structural basis of ribosome activity in peptide bond synthesis. *Science* **289:** 920–930.

Noller HF. 2005. RNA structure: Reading the ribosome. *Science* **309:** 1508–1514.

Noller HF, Kop J, Wheaton V, Brosius J, Gutell RR, Kopylov AM, Dohme F, Herr W, Stahl DA, Gupta R, et al. 1981. Secondary structure model for 23S ribosomal RNA. *Nucleic Acids Res* **9:** 6167–6189.

Noller HF, Hoffarth V, Zimniak L. 1992. Unusual resistance of peptidyl transferase to protein extraction procedures. *Science* **256:** 1416–1419.

Ogle JM, Brodersen DE, Clemons WM Jr, Tarry MJ, Carter AP, Ramakrishnan V. 2001. Recognition of cognate transfer RNA by the 30S ribosomal subunit. *Science* **292:** 897–902.

Orgel LE. 1968. Evolution of the genetic apparatus. *J Mol Biol* **38:** 381–393.

Ostergaard P, Phan H, Johansen LB, Egebjerg J, Ostergaard L, Porse BT, Garrett RA. 1998. Assembly of proteins an rRNA to transcripts of the major structural domains of 23S rRNA. *J Mol Biol* **284:** 227–240.

Rich A. 1962. On the problems of evolution and biochemical information transfer. In *Horizons in biochemistry* (ed. M Kasha, B Pullman), pp. 103–126. Academic, New York.

Samaha RR, O'Brien B, O'Brien TW, Noller HF. 1994. Independent in vitro assembly of a ribonucleoprotein particle containing the 3′ domain of 16S rRNA. *Proc Natl Acad Sci* **91:** 7884–7888.

Schuwirth BS, Borovinskaya MA, Hau CW, Zhang W, Vila-Sanjurjo A, Holton JM, Cate JH. 2005. Structures of the bacterial ribosome at 3.5 Å resolution. *Science* **310:** 827–834.

Selmer M, Dunham CM, Murphy FV, Weixlbaumer A, Petry S, Kelley AC, Weir JR, Ramakrishnan V. 2006. Structure of the 70S ribosome complexed with mRNA and tRNA. *Science* **313:** 1935–1942.

Sloof P, Van den Burg J, Voogd A, Benne R, Agostinelli M, Borst P, Gutell R, Noller H. 1985. Further characterization of the extremely small mitochondrial ribosomal RNAs from trypanosomes: A detailed comparison of the 9S and 12S RNAs from *Crithidia fasciculata* and *Trypanosoma brucei* with rRNAs from other organisms. *Nucleic Acids Res* **13:** 4171–4190.

Smith TF, Lee JC, Gutell RR, Hartman H. 2008. The origin and evolution of the ribosome. *Biol Direct* **3:** 16. doi: 10.1186/1745-6150-3-16.

Tumminia SJ, Hellmann W, Wall JS, Boublik M. 1994. Visualization of protein-nucleic acid interactions involved in the *in vitro* assembly of the *Escherichia coli* 50S ribosomal subunit. *J Mol Biol* **235:** 1239–1250.

Weitzmann CJ, Cunningham PR, Nurse K, Ofengand J. 1993. Chemical evidence for domain assembly of the *Escherichia coli* 30S ribosome. *FASEB J* **7:** 177–180.

Wilkinson KA, Merino EJ, Weeks KM. 2005. RNA SHAPE chemistry reveals nonhierarchical interactions dominate equilibrium structural transitions in $tRNA^{Asp}$ transcripts. *J Am Chem Soc* **127:** 4659–4667.

Wimberly BT, Brodersen DE, Clemons WM Jr, Morgan-Warren RJ, Carter AP, Vonrhein C, Hartsch T, Ramakrishnan V. 2000. Structure of the 30S ribosomal subunit. *Nature* **407:** 327–339.

Woese CR. 1967. *The genetic code: The molecular basis for genetic expression*. Harper & Row, New York.

Woese CR. 2001. Translation: In retrospect and prospect. *RNA* **7:** 1055–1067.

Woese CR, Magrum LJ, Gupta R, Siegel RB, Stahl DA, Kop J, Crawford N, Brosius J, Gutell R, Hogan JJ, et al. 1980. Secondary structure model for bacterial 16S ribosomal RNA: Phylogenetic, enzymatic and chemical evidence. *Nucleic Acids Res* **8:** 2275–2293.

Wolf YI, Koonin EV. 2007. On the origin of the translation system and the genetic code in the RNA world by means of natural selection, exaptation, and subfunctionalization. *Biol Direct* **2:** 14. doi: 10.1186/1745-6150-2-14.

Yusupov MM, Yusupova GZ, Baucom A, Lieberman K, Earnest TN, Cate JH, Noller HF. 2001. Crystal structure of the ribosome at 5.5 Å resolution. *Science* **292:** 883–896.